Supporting information

Unraveling the Nanosheet Zeolite-Catalyzed Combustion of Aluminum Nanoparticles-Doped exo-Tetrahydrodicyclopentadiene (JP-10) Energetic Fuel

Dababrata Paul[a], Souvick Biswas[a], Hyeonji Yeom[b], Kyungsu Na[b*], Michelle L. Pantoya[c*], Ralf I. Kaiser[a*]

[a] *Department of Chemistry, University of Hawai'i at Manoa, Honolulu, Hawaii 96822, USA*

[b] *Department of Chemistry, Chonnam National University, Gwangju 61186, South Korea*

[c] *Mechanical Engineering Department, Texas Tech University, Lubbock, Texas 79409, USA*

* Corresponding author. E-mail: ralfk@hawaii.edu

* Corresponding author. E-mail: kyungsu_na@chonnam.ac.kr

* Corresponding author. E-mail: michelle.pantoya@ttu.edu

Preparation of $C_{22\text{-}6\text{-}6}Br_2$ surfactant

The $C_{22\text{-}6\text{-}6}Br_2$ surfactant was synthesized as follows: 51.7 g (0.3 mol) of N,N,N',N'-tetramethyl-1,6-diaminohexane (> 98.0%, TCI) and 11.7 g (0.03 mol) of 1-bromodocosane (> 98.0%, TCI) were dissolved in 400 mL acetonitrile/toluene mixture (1:1 v/v) and magnetically stirred at 60°C for 12 h. The solvent was removed using a rotary evaporator at 45°C (120 rpm). To the residual solution, 400 mL of diethyl ether (DAEJUNG) was added, followed by cooling in a refrigerator. The precipitated product was filtered, washed with diethyl ether, and dried in a vacuum oven at 50°C. 14.0 g (0.025 mol) of the product and 8.4 g (0.05 mol) of 1-bromohexane (98%, Sigma-Aldrich) were dissolved in 300 mL acetonitrile and refluxed for 10 h. After cooling in a refrigerator, the product was filtered, washed with diethyl ether, and dried in a vacuum oven at 50°C.

Sample characterization

X-ray diffraction (XRD) patterns were obtained using a Rigaku MiniFlex 600 apparatus with Cu Kα radiation (λ=0.1541 nm) at 600 W (40 kV, 15 mA). All measurements were performed under ambient conditions with a step size of 0.05°, scanning rate of 4° min^{-1}, and 2θ range of 5-40°. Scanning electron microscopy (SEM) images were taken with a Gemini 500 (ZEISS, 3.0 kV) without a metal coating. Transmission electron microscopy (TEM) was performed using a JEM-2100F (JEOL Ltd.) instrument operating at 200 kV. N_2 adsorption isotherms were measured using a BELSORP MAX II volumetric analyzer at liquid N_2 temperature (77 K). Before the measurements, samples were degassed at 350 °C under vacuum for 4 h. The surface areas were calculated according to the Brunauer-Emmett-Teller (BET) theory. The average pore diameter and total pore volume were determined from the desorption branch of the isotherm using the Barrett-Joyner-Halenda (BJH) algorithm. The pore diameter was calculated from the desorption branch of the isotherm using the BJH technique, with a 20% error[1]. Elemental analyses were performed by ICP-OES using an Optima 8300 (PerkinElmer). The NH_3-TPD profiles of the NSMFI(y) zeolites exhibits two distinct desorption peaks at ~180°C and ~360-390°C, assigned to weak and strong acid sites, respectively[2-4]. These NH_3-TPD results show that NSMFI(60) has the highest acid sites. As the Si/Al ratios of zeolites increase, the number of acid sites decreases and their strength decreases.

Raman spectroscopy

The Raman spectra of each NSMFI(y) zeolites as well as droplets were collected by using home built Raman spectrometer prior to ignition. A laser beam (Q-switched Nd:YAG laser, model: QL532-1W0) having a beam diameter of 0.35 mm and a divergence angle of 3.8 mR was introduced into the chamber through an antireflection coated window from a mirror (Edmund Optics, model NT45-991, 499% reflectance) followed by a dichroic beam splitter (Semrock, RazorEdge, model LPD01-532RU-25 × 36 × 2.0). A plano-convex lens with a focal length of 60 mm focused the laser beam onto the droplet with a diameter of approximately 20 μm. The Raman shifted photons, backscattered from the droplet are then passed through an ultra-steep long-pass edge filter (Semrock, model LP03-532RE-25) which cuts down the elastically scattered 532 nm laser light. The resultant backscattered photons were collected via holographic imaging spectrograph (Kaiser Optical Systems, model 2004500-501 and Holoplex HPG-532), equipped with a PI-Max 2 ICCD camera (Princeton Instruments). The resolution of the Raman spectrometer is 9 cm^{-1}. The excitation laser and detector both operate at a repetition rate of 1 kHz and are externally driven and synced by a pulse generator (Quantum Composer Plus, model-9518). The Raman spectrometer was calibrated by recording Raman spectra from levitating reference droplets of cyclohexane (C_6H_{12}), toluene ($C_6H_5CH_3$), and acetonitrile (CH_3CN).

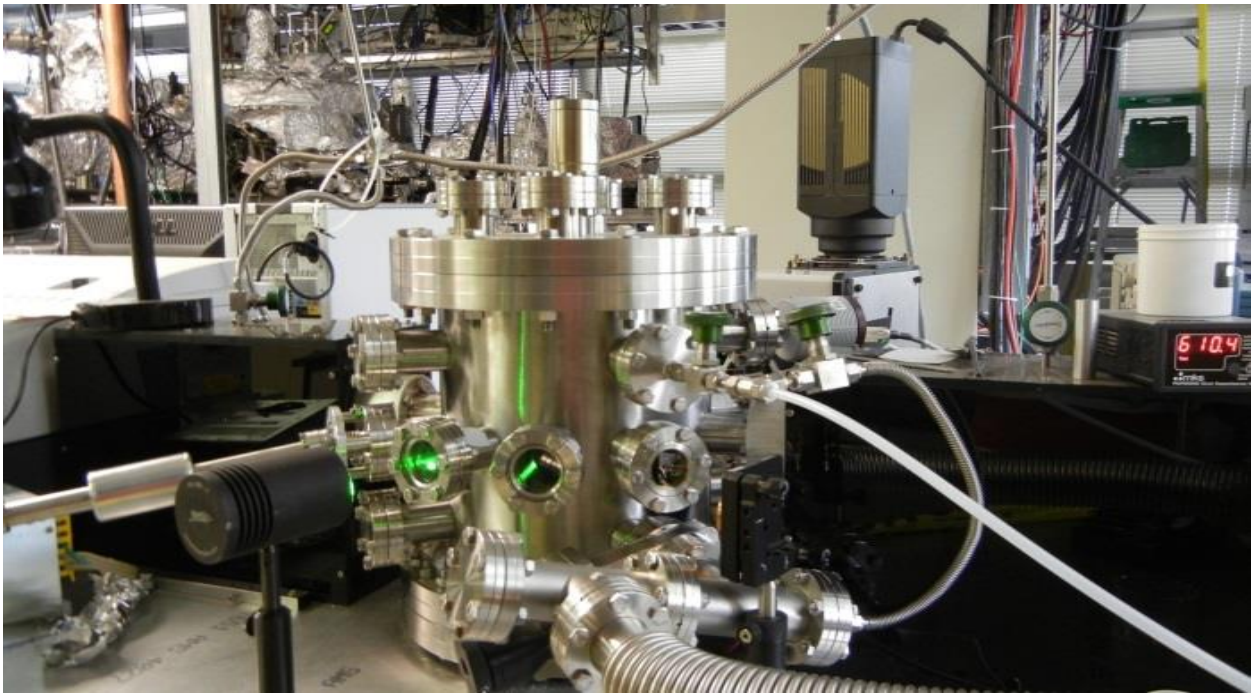

Figure S1. Side view of the levitator experimental setup exploiting the levitation device.

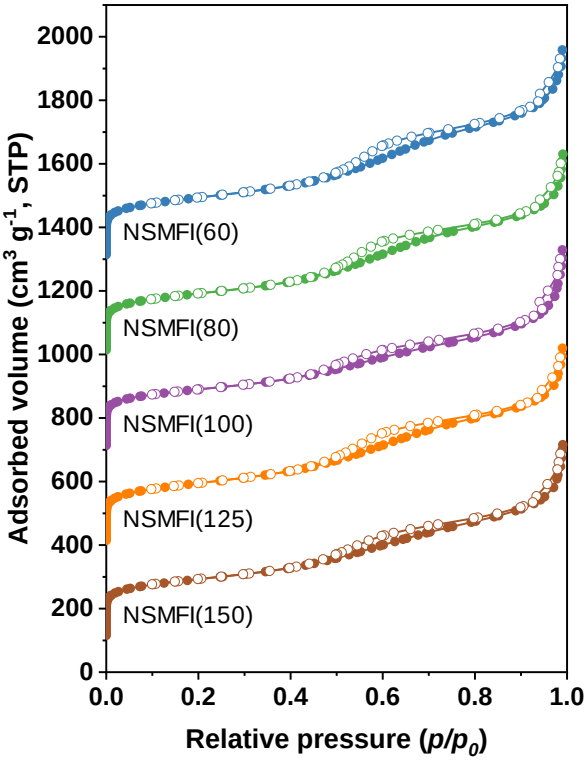

Figure S2. The N_2 adsorption isotherms of the as-synthesized five nanosheet MFI zeolites: NSMFI(60), NSMFI(80), NSMFI(100), NSMFI(125), and NSMFI(150) with controlled Si/Al ratio.

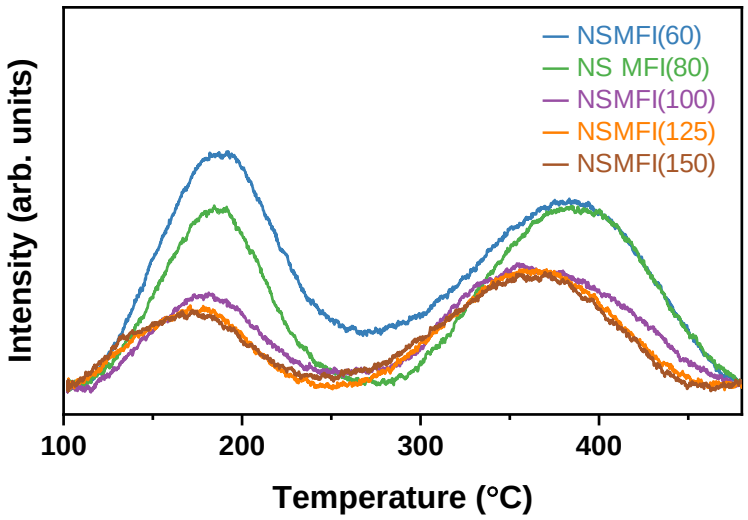

Figure S3. NH_3-TPD profiles of the NSMFI(y) zeolites.

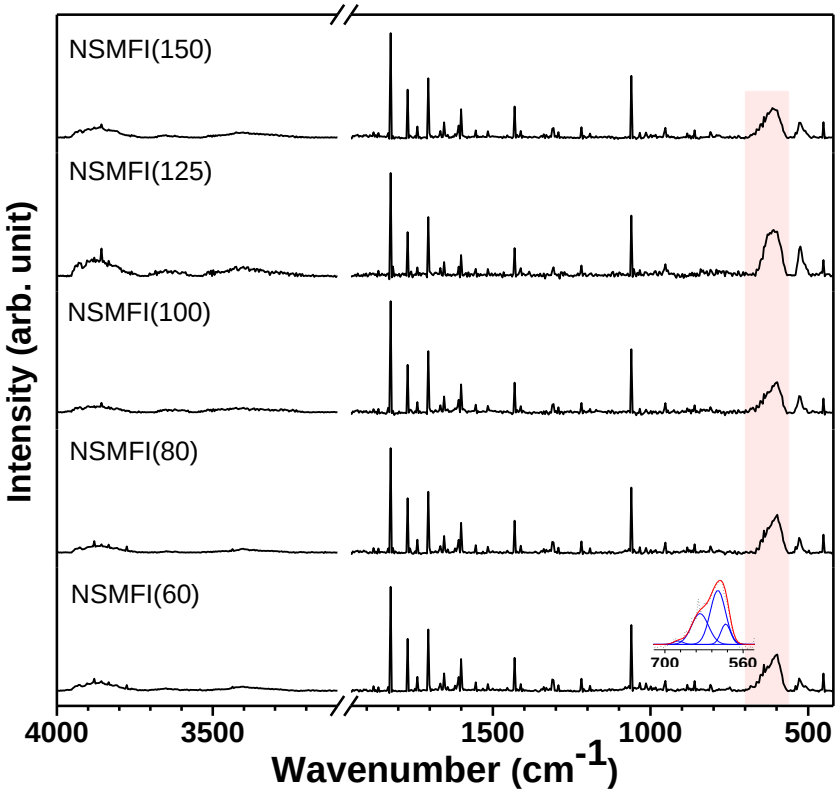

Figure S4. Raman spectra of five nanosheet MFI zeolites: NSMFI(60), NSMFI(80), NSMFI(100), NSMFI(125), and NSMFI(150) with controlled Si/Al ratios. The peaks and bands of NSMFI zeolites are assigned and listed in Table S1.

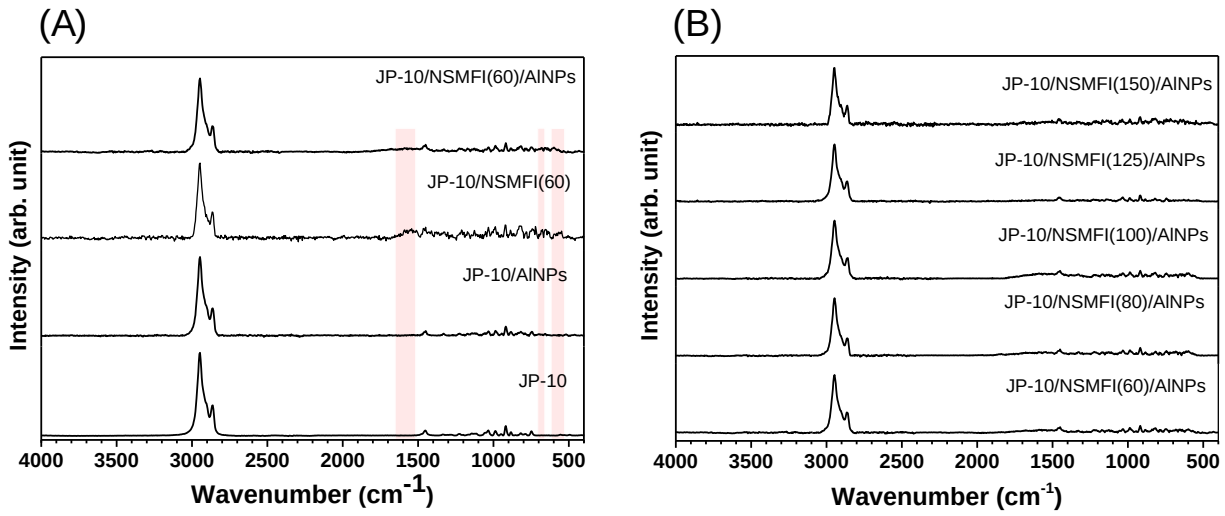

Figure S5. Raman spectra of JP-10, JP-10/AlNPs, JP-10/NSMFI(60), and JP-10/NSMFI(60)/AlNPs are shown in (A), and JP-10 doped with NSMFI(60)/AlNPs, NSMFI(80)/AlNPs, NSMFI(100)/AlNPs, NSMFI(125)/AlNPs, and NSMFI(150)/AlNPs are shown in (B). The bands of JP-10, JP-10/AlNPs, JP-10/NSMFI, and JP-10/NSMFI/AlNPs are assigned and listed in Table S2.

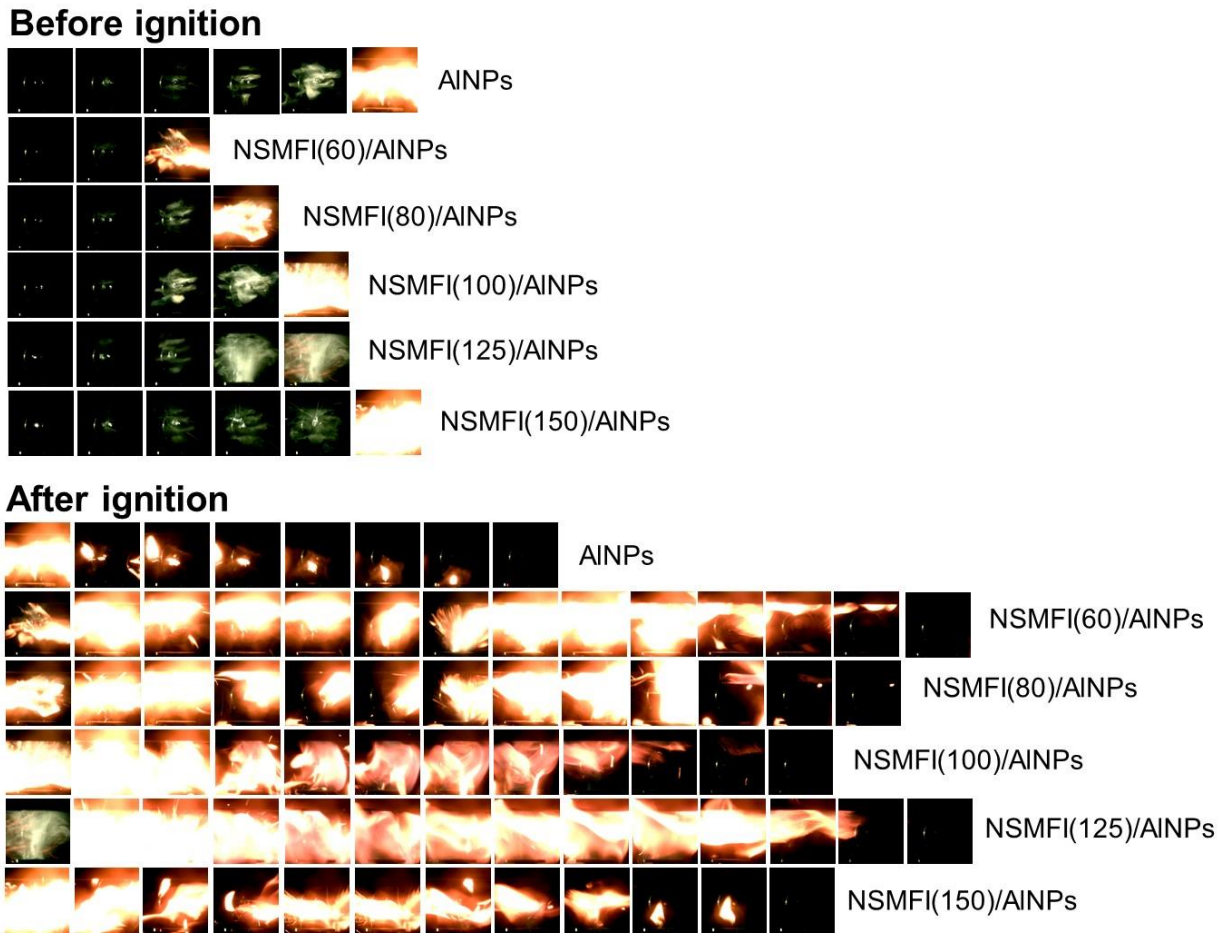

Figure S6. Time resolved optical images recorded in the combustion of JP-10 droplets doped with AlNPs, NSMFI(60)/AlNPs, NSMFI(80)/AlNPs, NSMFI(100)/AlNPs, NSMFI(125)/AlNPs, and NSMFI(150)/AlNPs ignitions. The images displayed here have a 5 ms interval.

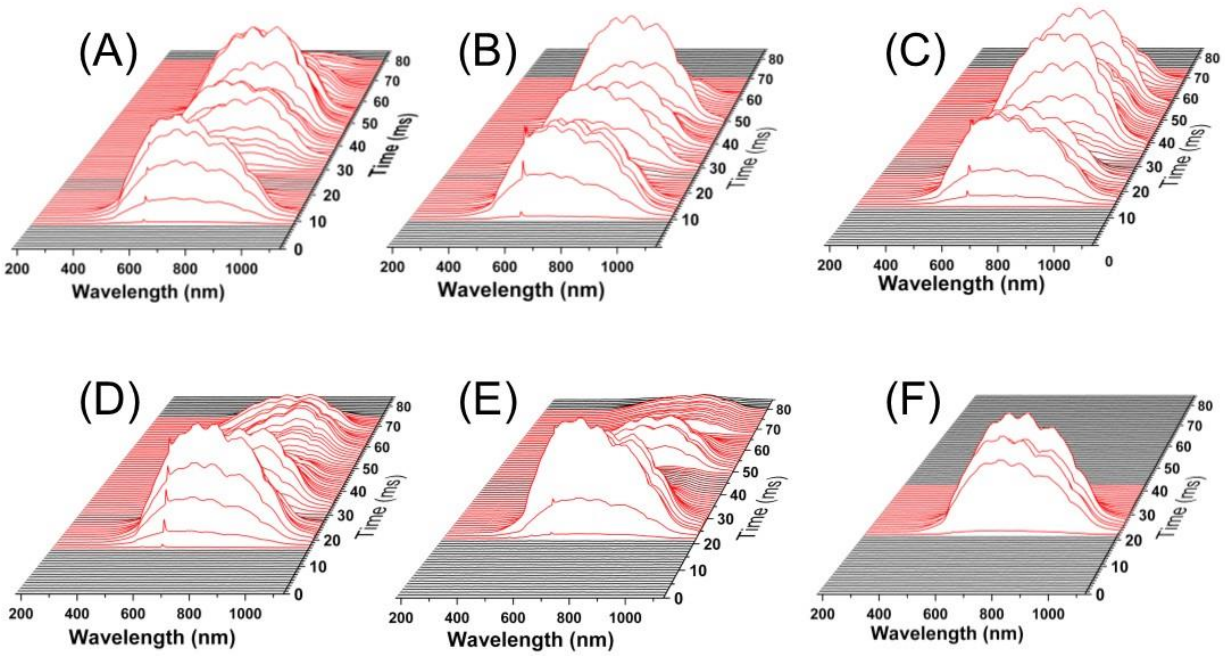

Figure S7. 3D plots of UV-vis emission spectra of JP-10 droplets doped with NSMFI(60)/AlNPs, NSMFI(80)/AlNPs, NSMFI(100)/AlNPs, NSMFI(125)/AlNPs, NSMFI(150)/AlNPs and AlNPs ignitions are presented (A-F).

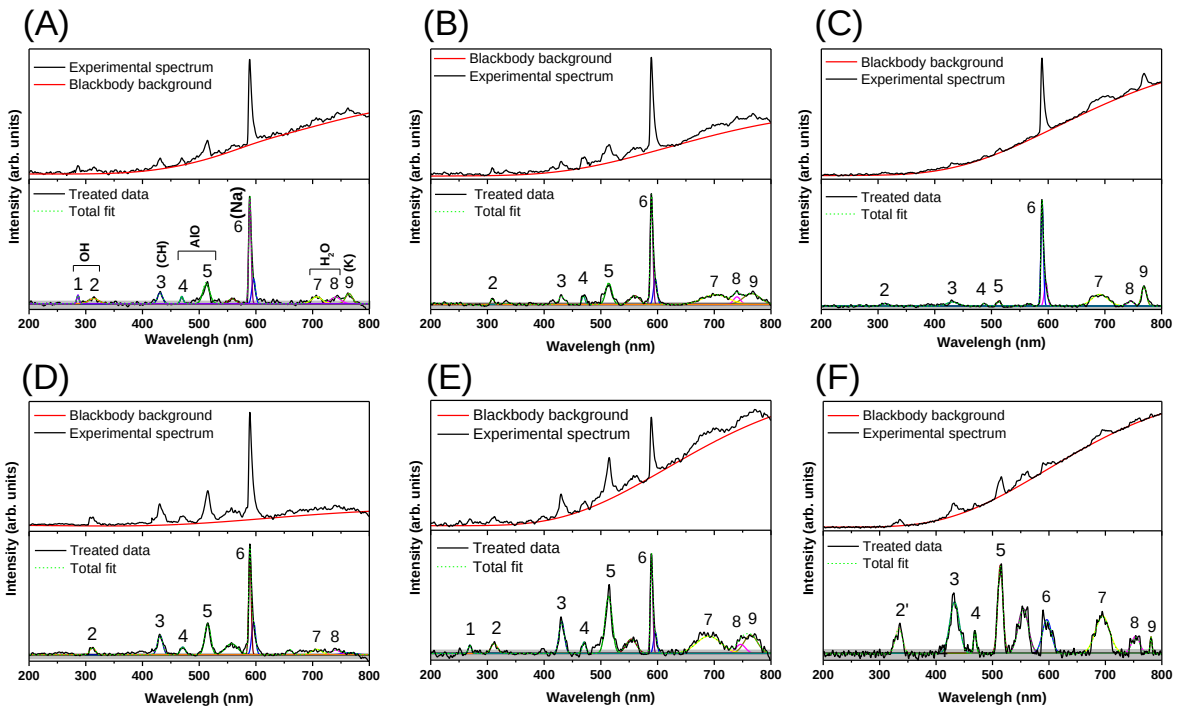

Figure S8. Deconvoluted UV-vis emission spectra of JP-10 droplets doped with NSMFI(60)/AlNPs, NSMFI(80)/AlNPs, NSMFI(100)/AlNPs, NSMFI(125)/AlNPs, NSMFI(150)/AlNPs and AlNPs ignitions are presented (A-F). The bands of JP-10 ignition by NSMFI zeolites and/or AlNPs are leveled in (A).

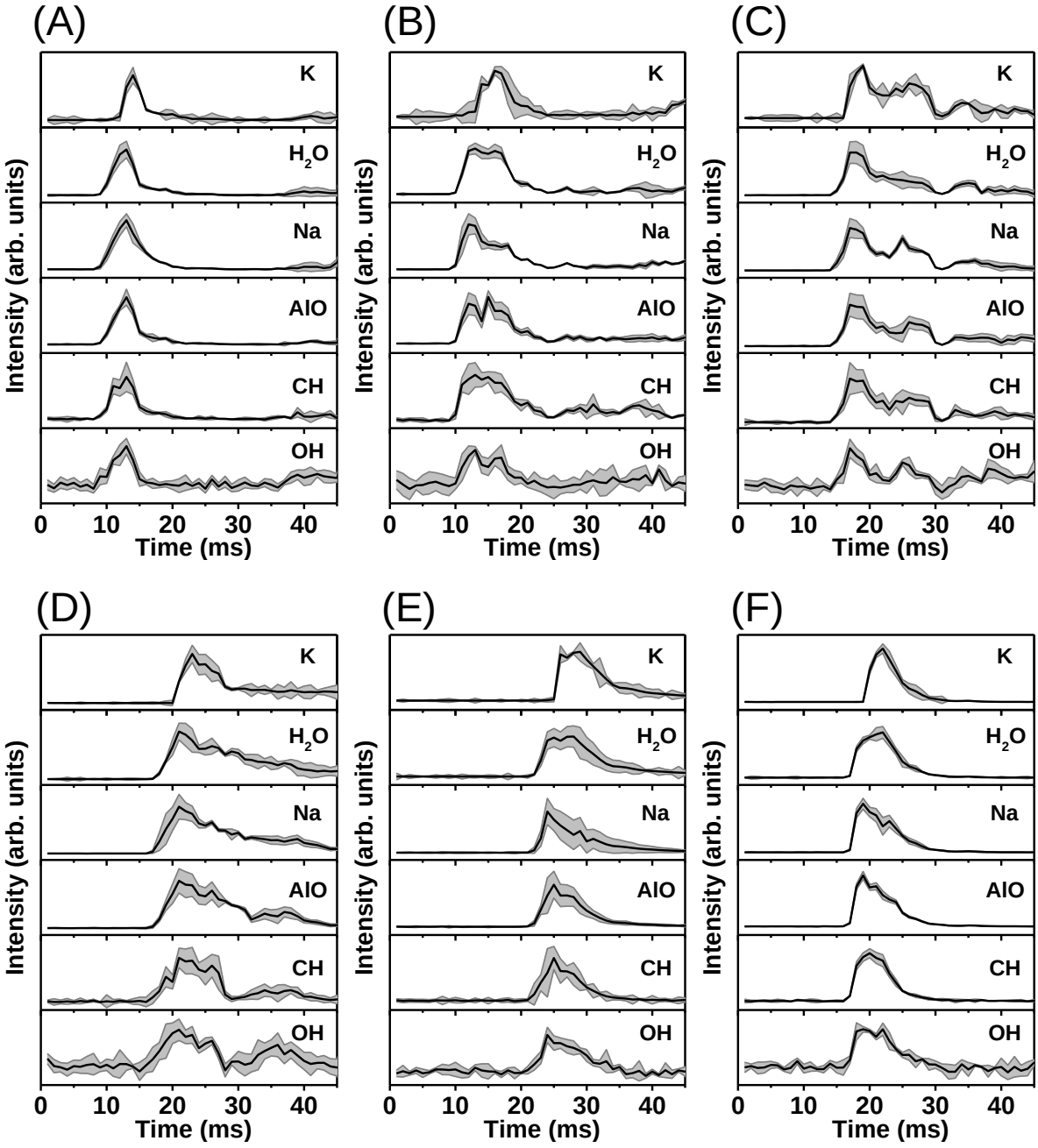

Figure S9. Temporal profiles of hydroxyl (OH), methylidene (CH), aluminum monoxide (AlO), sodium (Na), water (H_2O), and potassium (K) produced during the combustion of (A) JP-10/NSMFI(60)/AlNPs, (B) JP-10/NSMFI(80)/AlNPs, (C) JP-10/NSMFI(100)/AlNPs, (D) JP-10/NSMFI(125)/AlNPs, (E) JP-10/NSMFI(150)/AlNPs and (F) JP-10/AlNPs droplets.

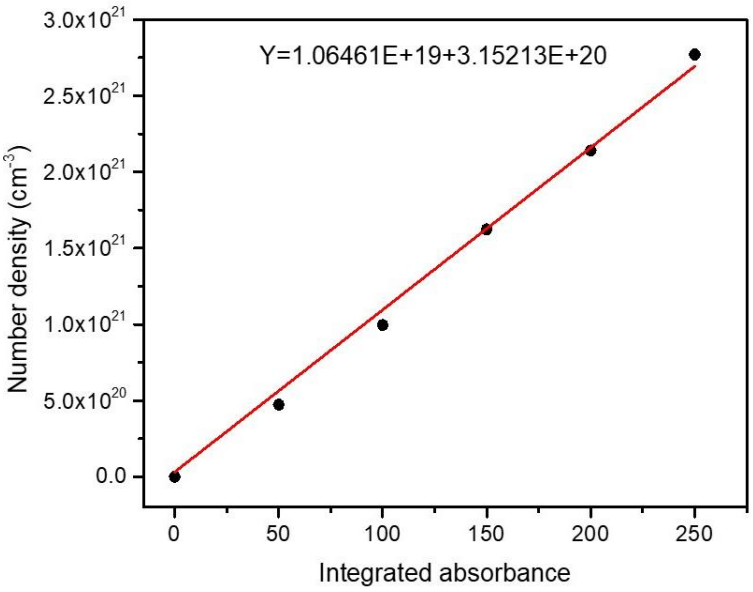

Figure S10. Calibration of FTIR signal for carbon dioxide (CO_2). Integrated area for the CO_2 antisymmetric stretch band in the 2170-2460 cm^{-1} range was used.

Table S1. Acidity content of NSMFI(y) zeolites.

Samples	Adsorbed NH_3 (mmol g^{-1})		
	Weak acid	Strong acid	Total
NSMFI(60)	0.009	0.011	0.020
NSMFI(80)	0.006	0.008	0.014
NSMFI(100)	0.003	0.007	0.010
NSMFI(125)	0.003	0.006	0.009
NSMFI(150)	0.003	0.006	0.009

Table S2. Raman peaks or bands of NSMFI zeolites.

Mode	Raman wavenumber (cm^{-1})		Vibrational mode
	NSMFI	Ref. band	
ν_1	451	454	δ (O-Si-O(Al))
ν_2	478	470	δ (Si-O)
ν_3	540	548	D5R
ν_4	588	590	ν_s (Al-O-Si)
ν_5	597	598	ν (Al-O-Si)
ν_6	630	617	D4R
ν_7	682	673	δ (Si-O-Al)
ν_8	748	745	ν (Si-O-Al)
ν_9	809	800	ν_s (Si-O-Si)
ν_{10}	860	832	ν (Al-O)
ν_{11}	883	890	δ (O-Si-H)
ν_{12}	960	967	ν_{as} (Al-O-H)
ν_{13}	1020	1028	ν_{as} (Si-O-Si)
ν_{14}	1070	1086	ν_{as} (Si-O-Si)
ν_{15}	1218		D4R + ν_s (Al-O-Si)
ν_{16}	1312		δ (Si-O-Al) + D4R
ν_{17}	1436		ν_s (Si-O-Si) + D4R
ν_{18}	1517		ν_{as} (Si-O-Si) + δ (O-Si-O(Al))
ν_{19}	1554		(Al-O) + δ (Si-O-Al)
ν_{20}	1600		(Al-O) + ν (Si-O-Al)
ν_{21}	1670		(Al-O) + ν_s (Si-O-Si)
ν_{22}	1704		ν_{as} (Si-O-Si) + D4R
ν_{23}	1770		ν_{as} (Al-O-H) + ν_s (Si-O-Si)
ν_{24}	1818		ν_{as} (Si-O-Si) + ν (Si-O-Al)
ν_{25}	3410		ν (OH in Si(OH)Al)
ν_{26}	3650		ν (O-H in H_2O)
ν_{27}	3870		ν (O-H in SiOH)

Table S3. Raman peaks or bands of JP-10 and JP-10 containing AlNPs, NSMFI, and NSMFI/AlNPs.

Mode	Raman wavenumber (cm^{-1})					Vibrational mode
	JP-10	JP-10 /AlNPs	JP-10 /NSMFI	JP-10 /NSMFI/AlNPs	Ref. band	
1	2947	2947	2947	2947	2954	Stretching (CH)
2	2903	2903	2903	2904	2910	Stretching (CH_2)
3	2863	2863	2862	2863	2870	Stretching (CH)
4	1475	1475	1476	1475	1465	Scissoring (CH_2)
5	1453	1453	1453	1453	1444	Scissoring (CH_2)
6	1427	1427	1428	1427	1420	Rocking (CH_2)
7	1330	1330	1329	1327	1327	Wagging (CH_2)
8	1303	1303	1303	1303	1304	Wagging (CH_2)
9	1278	1278	1278	2172	1276	Wagging (CH_2)
10	1226	1226	1226	1226	1219	Bending (CH_2)
11	1201	1201	1202	1202	1196	Wagging (CH_2)
12	1166	1172	1172	1172	1161	Twisting (CH_2)
13	1143	1143	1144	1144	1138	Twisting (CH_2)
14	1127	1127	1127	1127	1126	Wagging (CH_2)
15	1113	1113	1113	1113	1107	Twisting (CH_2)
16	1056	1056	1058	1058	1050	Rocking (CH_2)
17	1033	1033	1033	1033	1030	Twisting (CH_2)
18	985	986	986	986	980	Stretching (CC)
19	948	945	945	945	945	Ring breathing
20	918	918	918	918	914	Ring stretching
21	883	884	883	884	879	Rocking (CCC)
22	854	853	854	853	853	Bending (CCC)
23	817	818	818	818	814	Rocking (CH_2)

24	787	787	788	788	783	Stretching (CC)
25	748	744	743	747	744	Stretching (CC)
26	555	556	556	555	551	Bending (CCC)
27	532	532	533	534	532	Ring twisting
28	493	494	493	494	490	Bending (CCC)
29	412	413	413	413	401	Bending (CCC)

Table S4. Vibrational mode assignments for the peaks and bands of gaseous products during ignition of JP-10 droplets doped with (A) AlNPs, (B) NSMFI(60)/AlNPs, (C) NSMFI(80)/AlNPs, (D) NSMFI(100)/AlNPs, (E) NSMFI(125)/AlNPs, and (F) NSMFI(150)/AlNPs through FTIR analysis.

Band	**Peak or band wavenumber (cm^{-1})**	**Molecule**	**Ref. band (cm^{-1})**	**Vibrational mode**
a	3750-3900	H_2O	3760	$\nu_{as}(H_2O)$
b	3715	CO_2	3714	Combination band
c	3614	CO_2	3612	Combination band
d	2955	$C_{10}H_{16}$	2956	$\nu(CH)$
e	2929	$C_{10}H_{16}$	2929	$\nu(CH_2)$
f	2877	$C_{10}H_{16}$	2879	$\nu(CH)$
g	2363	CO_2	2359	$\nu_{as}(CO_2)$
h	2339	CO_2	2347	$\nu_{as}(CO_2)$
i	2273	$^{13}C^{16}O_2$	2279	$\nu_{as}(CO_2)$
j	1500-1750	H_2O	1600	$\delta(OH)$
k	1467	$C_{10}H_{16}$	1467	Scissoring (CH_2)
l	668 651 720, 680, 659, 617	CO_2 $^{13}C^{16}O_2$ CO_2	668 648 720,680,655,619	$\delta(CO_2)$ $\delta(CO_2)$ $\delta(CO_2)$

References

(1) Fu, S.; Fang, Q.; Li, A.; Li, Z.; Han, J.; Dang, X.; Han, W. Accurate Characterization of Full Pore Size Distribution of Tight Sandstones by Low-Temperature Nitrogen Gas Adsorption and High-Pressure Mercury Intrusion Combination Method. *Energy sci. eng.* **2021**, *9*, 80.
(2) Li, C.; Wang, J.; Gao, G.; Zhao, Z.; Sun, P.; Li, F. Enhanced Stability of Hierarchical Zeolite-Metal Bifunctional Catalysts for Conversion of Levulinic Acid to Valeric Biofuels. *Chem. Eng. J.* **2024**, *483*, 149405.
(3) Sadowska, K.; Wach, A.; Olejniczak, Z.; Kuśtrowski, P.; Datka, J. Hierarchic Zeolites: Zeolite ZSM-5 Desilicated with NaOH and NaOH/Tetrabutylamine Hydroxide. *Microporous Mesoporous Mater.* **2013**, *167*, 82.
(4) Mishra, S.; Ali Haider, M.; Pant, K. K. Controlling the Evolution of Active Molybdenum Carbide by Moderating the Acidity of Mo/HMCM-22 Catalyst in Methane Dehydroaromatization. *Catal. Letters* **2020**, *150*, 3653.